International Journal of Applied Engineering and Technology ISSN: 2277-212X (Online)
An Open Access, Online International Journal Available at http://www.cibtech.org/jet.htm
2016 Vol. 6 (3) July-September, pp.107-115/Kumar
Research Article

INVESTIGATION ON THE EFFECTS OF ELLIPSOIDAL TEXTURES ON THE PERFORMANCE OF POROUS JOURNAL BEARING

***R. Kumar**
Department of Mechanical Engineering, Arni University – Kathgarh, Indora, Kangra (H.P.)- India
**Author for Correspondence*

ABSTRACT
The present study reveals the investigation on the effects of ellipsoidal textures on the performance of porous journal bearing. The modified Reynolds equation with Darcy equation and equations accounting for surface texturing is mathematically derived for porous journal bearing. The Darcy's equation is used to account for the effects of porous region of the bearing. The modified Reynolds equation is solved numerically through finite difference approach and Simpson's 1/3rd method and over relaxation methods are used in computing the various bearing characteristics by changing various bearing parameters such as eccentricity ratio, shaft speed, dimple depth and permeability parameter. The ellipsoidal type of surface textures are incorporated on the bearing surface for finding the influence on the performance characteristics of finite porous journal bearing. It is observed that the textures on the bearing characteristics give pronounced results as compared to the smooth case. The dimple depth also plays an important role in investigation of the performance as with increase in dimple depth the load carrying capacity increases. The permeability parameter reduces the load carrying capacity and reduction is more in case of large values.

Keywords: *Porous Journal Bearing; Surface Texture; Finite Difference Method; Ellipsoidal Dimples*

INTRODUCTION
Many researchers have adopted different techniques for analyzing hydrodynamic journal bearing's performance. Various parameters such as type of roughness (random or Deterministic), nature of lubricant i.e., Newtonian or non-Newtonian, and the shape of the bearing (elliptical or two and three lobe) etc. have been considered for investigation by researchers in past. The performance of hydrodynamic bearings is numerically computed through Reynolds equation for Newtonian fluids. Journal bearings are generally used in heavy machinery, where these bearings operate at high-speeds and there is a possibility of shear thinning of the fluid. At this time, the Reynolds equation may not be capable for predicting accurate pressures etc. furthermore commercial lubricants behave like non-Newtonian lubricants, due to the presence of different types of additives, which leads to the application of non-Newtonian theory to various lubrication problems. The need to reduce friction and the amount of wear on machine element components involved in sliding contact is ever present. The efficiency, reliability, and durability of such components depend on the friction that occurs at the sliding contact interface. In addition, there is always the desire to increase the load capacity or the power density of machine elements, which of course will lead to higher severity of surface interaction. Both the need to reduce friction and the desire to increase load capacity require effective lubrication strategy for sliding surfaces.
With the development of modern machines, the use of various fluids as lubricants under various circumstances has been given much importance. Most bearings are normally used to support rotating shafts in machines. Appropriate bearing design can minimize friction and wear as well as early failure of machinery.
The objectives of bearing design are to extend bearing life in machines, reduce friction energy losses and wear, and minimize maintenance expenses and downtime of machinery due to frequent bearing failure. In manufacturing plants, unexpected bearing failure often causes expensive loss of production. The classification of bearing includes the rolling element bearing, hydrostatic, hydrodynamic and magnetic bearing. Hydrodynamic bearings are used in various machines ranging from small engines to large turbines or in turbo machinery and these are operated at very high loads and speeds. At these operating

conditions, friction losses are more, it means lubricant and bearing temperature becomes too high which becomes a serious problem (Hori, 2006; Cameron, 1966; Khonsari and Booser, 2001; Hamrock *et al.*, 2004).

Hydrodynamic lubrication is generally characterized by conformal surfaces. A positive pressure develops in a hydro dynamically lubricated journal or thrust bearing because the bearing surfaces converge and the relative motion and the viscosity of the fluid separate the surfaces. The existence of this positive pressure implies that a normal applied load may be supported. The magnitude of the pressure developed (usually less than 5 MPa) is not generally large enough to cause significant elastic deformation of the surfaces. The minimum film thickness normally exceeds 1μm in hydrodynamic lubrication where the films are generally thick so that opposing solid surfaces are prevented from coming into contact. This condition is often referred to as "the ideal form of lubrication" since it provides low friction and high resistance to wear. Positive pressures will be generated only when the film thickness is diminishing. For a normal load to be supported by bearing, positive-pressure profiles must be developed over the bearing length. Most of the machinery used in modern industry strongly demands the use of environmentally conscious or energy-efficient components, including various moving small components, which are directly or indirectly in contact with each other. The resulting friction and wear at the contact–sliding interface may be the most important factor affecting the energy efficiency for these moving components (Kango and Sharma, 2010; [Online]; Kumar, 1980; Morgan and Cameron, 1957; Rouleau and Steiner, 1974; Murti, 1973).

Surface texturing technology is one prominent method to reduce friction and wear and thus, improves the energy efficiency, by changing lubrication characteristics at the interface between the components in relative movement. Maintaining appropriate lubrication on a sliding surface can be accomplished by using a porous material. In the oil impregnated bearings widely used in many machines where longevity is sought, a thin porous layer is coated on the bearing surface to reserve excessive oil and enhance the bearing reliability. A number of authors work on the texturing aspects of bearings (Prakash and Tiwari, 1982; Prakash and Tiwari, 1983; Reason and Sew, 1985; Naduvinamani and Patil, 2009; Naduvinamani *et al.*, 2002; Gururajan and Prakash, 1999; Tala-Ighil *et al.*, 2007; Kango *et al.*, 2012; Kango *et al.*, 2014; Sharma *et al.*, 2014; Sharma *et al.*, 2014). In the present work, ellipsoidal types of dimples are incorporated on the bearing surface on a particular location and performance is investigated.

Mathematical and Computational Procedure

The Reynolds equation for an incompressible, Iso-viscous fluid rheology of the bearing system for a combination of flow in the bearing clearance and that within the porous wall is given by Cameron, (1983). Figure 1 shows the schematic diagram for a plain journal bearing.

The circumferential length in the x-direction is rθ, the porous bearing length in the axial direction is L and nominal film thickness in the radial direction is *h*. The origin is taken on the oil sinter interface. The sinter is of thickness H, extending down to y = -H, and has a permeability Ø. The journal moves at a surface velocity U and the oil film thickness can be given as:

$$h = C_r(1 + e\cos\theta)$$

The flow through the sinter was governed by Darcy's law which can be given mathematically as

$$w = -\frac{\partial p}{\partial y}\frac{\phi}{\eta}$$

There is a negative sign as the flow is in decreasing pressure. The equation of continuity of flow is given as.

$$\frac{\partial}{\partial x}\left(h^3\frac{\partial p}{\partial x}\right) + \frac{\partial}{\partial z}\left(h^3\frac{\partial p}{\partial z}\right) = 6\eta\left[U\frac{dh}{dx} - 2\left(\frac{\partial^2 p}{\partial x^2} + \frac{\partial^2 p}{\partial z^2}\right)\frac{\phi H}{\eta}\right] \quad (1)$$

Equation (1) is the generalized Reynolds equation for porous journal bearing.

Figure 2 depicts the geometry for ellipsoidal dimple supposed on the bearing surface in the present work. The mathematical model for ellipsoidal texture is also adopted from the work of previous authors. The work of ellipsoidal texture incorporated on the bearing surface is adopted from Kango *et al.*, (2014).

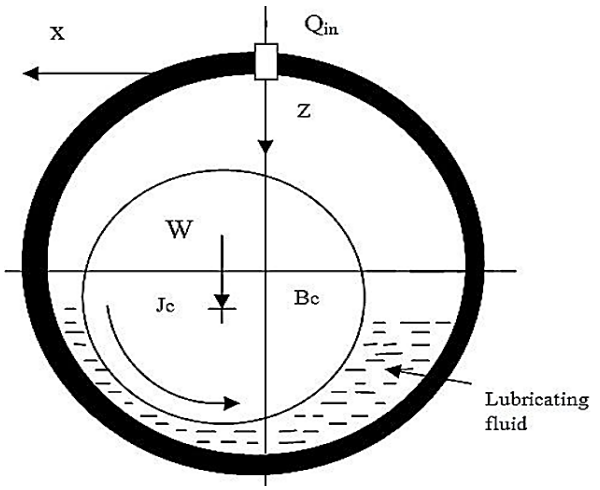

Figure 1: Schematic Diagram of a Journal Bearing

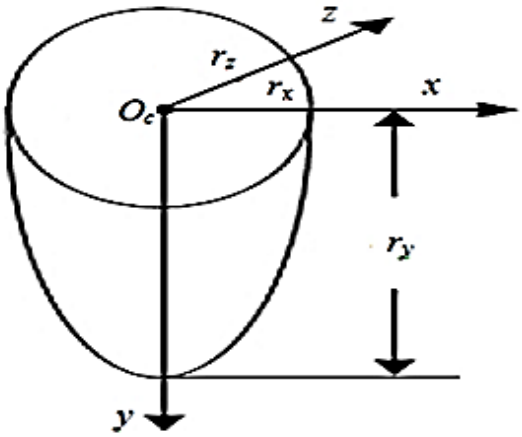

Figure 2: Geometry of Ellipsoidal Dimple

The three dimensional geometry of an elliptical dimple is taken from Kango *et al.*, (2014) and as follows:

$$\left(\frac{(x-x_c)^2}{r_x^2}+\frac{(y-y_c)}{r_y^2}+\frac{(z-z_c)^2}{r_z^2}\right)=1$$

r_x, r_y and r_z are the radii of the ellipsoidal dimples in the x, y and z directions respectively. The expressions for x, x_c and z_c are also adopted from Kango *et al.*, (2014).

$$x=R\theta,\ x_c=n_1a+\frac{(2n_1-1)L_x}{2},\quad z_c=n_1b+\frac{(2n_1-1)L_z}{2}$$

where, n_1 is the number of dimples and a and b are the distances.

With the help of above equations,

$$\Delta h_{eps}=r_y\times\sqrt{(1.0-r_{eps})}$$

$$r_y=\left(\frac{(R\theta-x_c)^2}{r_x^2}+\frac{(z-z_c)^2}{r_z^2}\right)$$

The film thickness equation for textured (dimpled) journal bearing is presented in equations as given below:

$$H_{texture}=C_r\ (1+\varepsilon\cos\theta)+\ \Delta h_{eps}$$

$H_{texture}$ is the film thickness for dimpled (ellipsoidal) bearing, ε denotes the eccentricity ratio, Δh_{eps} is the dimensionless film thickness component and measures of ellipsoidal respectively, on the bearing surface.

The boundary conditions for the Reynolds equation for the smooth and rough bearings are:

$$p=0\ \text{At}\ \theta=0^0,360^0$$

$$p=0\ \text{And}\ \frac{\partial p}{\partial\theta}=0\ \text{ at }\ \theta=\theta_c$$

Where θc corresponds to initiation of cavitation.

The load carrying capacity can be obtained by the following expressions.

$$w_2=\int_0^l\int_0^{2\pi}pr\cos\theta d\theta dz$$

$$w_2 = \int_0^l \int_0^{2\pi} pr \sin\theta d\theta dz$$

$$w = \sqrt{{w_1}^2 + {w_2}^2}$$

For the numerical solution of the derived modified Reynolds equation, the finite difference scheme has been used. In finite difference scheme, the differential equation has been solved numerically on the grid point notation. The first order derivative and second order derivative has been discretized by second order central difference.

The convergence criteria for the derived equations can be taken as given below:

$$\sum\sum \left| \frac{\left(P_{I,J} - P(I,J)_{K-1} \right)}{P(I,J)_K} \right| < 0.0001$$

Where *I, J* denotes the number of nodes and k denotes the number of iterations respectively. For this work, we used 150 nodes in x- direction and 48 nodes in z-direction. The pressure is computed iteratively through Gauss- Seidel method and over relaxation factor is used for finding solutions. In this program, the over relaxation factor is taken as 1.4-1.5. We also represent the algorithm and the flow chart for these numerical computations.

RESULTS AND DISCUSSION

In this section, the mathematical models which were derived (the Reynolds equation and texture equations) in previous chapter are utilized for the numerical analysis. The input data has been taken from the previous studies performed by different authors and have calculated the various bearing performance characteristics viz. fluid film pressures, load carrying capacity etc.

Table 1: Input Data

Input Data	Input Value
Eccentricity ratio(ε)	0.1-0.5
Shaft speed(N), rpm	1000, 2000
Radial Clearance(C_r), m	50 x 10^{-6}
Shaft Radius(R), m	0.02
Bearing length(L), m	0.04
Consistency parameter at inlet temperature (m_0), Pa-s	0.08
Nodes in circumferential direction (N_θ)	223
Permeability parameter (ψ)	0, 0.005, 0.01, 0.05,0.1
Nodes in axial direction (N_z)	72
$d\theta$, m	0.000566
dz, m	0.000566
Dimple radius(r_s), m	0.003
Elliptic radius (r_x and r_z), m	0.0015 and 0.003
Dimple depth(r_y), µm	10, 20,30,40
L_x,m	0.0076
L_z, m	0.0076
a	0.001132
b	0.001689
Number of dimples in circumferential direction (N_{tx})	5
Number of dimples in axial direction (N_{tz})	4

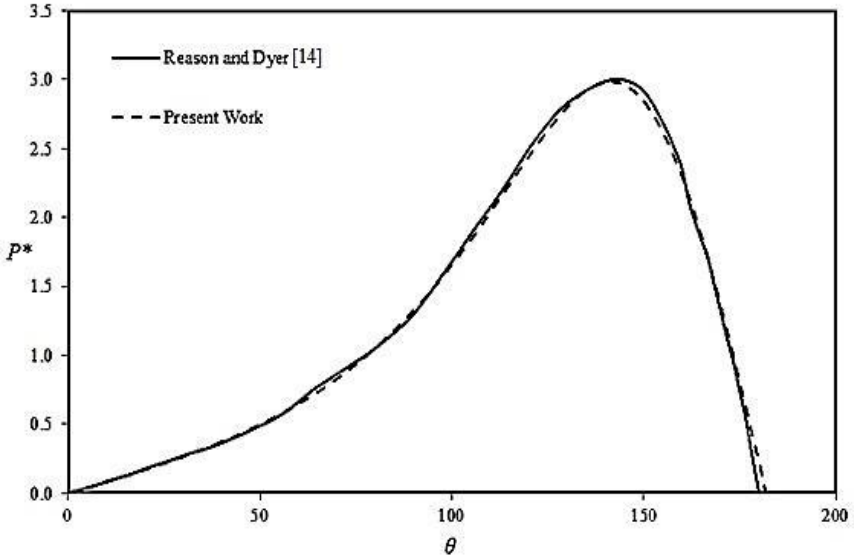

Figure 3 Validation of Dimensionless Mid Plane Pressure P* Distribution as a Function of (θ) with the Work of Reason and Dyer (Naduvinamani and Patil, 2009)

Figure 3 shows the validation of present work with the work of Reason and dyer (Naduvinamani and Patil, 2009) for fluid film pressure distribution and the trends clearly shows the equitably matching with the present model.

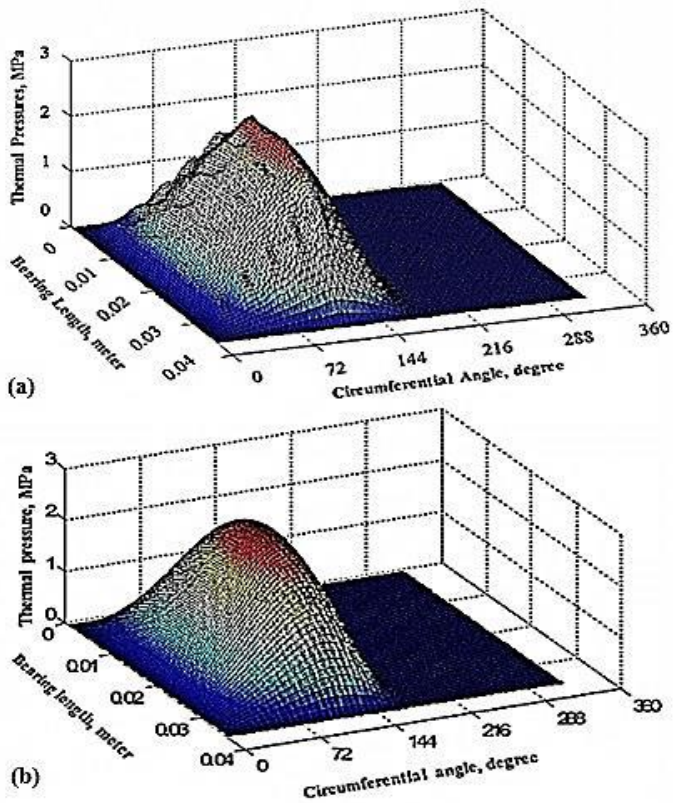

Figure 4: Three Dimensional Representations for Variation of Fluid Film Pressure in Case of (a) Ellipsoidal Dimple (Textured Surface) and (b) Smooth Surface

The test performed on numerical results arriving on the number of nodes (150 × 48 grids) and error (10^{-4}) have adopted in this computation. Results clearly reveal that texturing enhances the performance. The enhancement in performance also reveals in Figure 4 which shows a three dimensional representation of comparison between smooth and textured (ellipsoidal dimples) bearing for variation of fluid film pressures. The fluid film pressures are significantly higher in textured case while compared with smooth case.

Figure 5 shows the effects of dimple depth on the load carrying capacity for the considered textures. The dimple depth is varied from 10 to 40 microns and load carrying capacity is calculated. It has been obtained that the load carrying capacity gets increased with increase in dimple depth. The results shown here are for low shaft speed (1000 rpm).

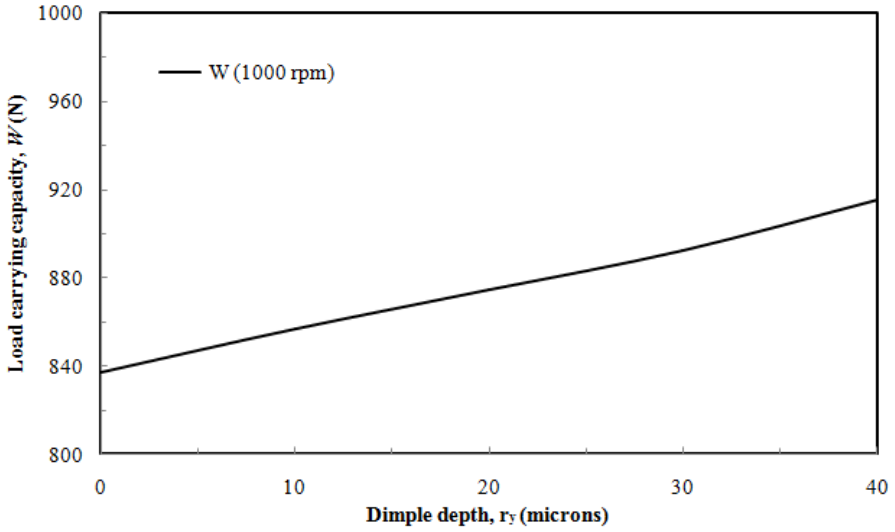

Figure 5: Effect of Dimple Depth on the Load Carrying Capacity of a Textured Porous Journal Bearing at Low Shaft Speed (*N*= 1000 rpm, ε=0.3)

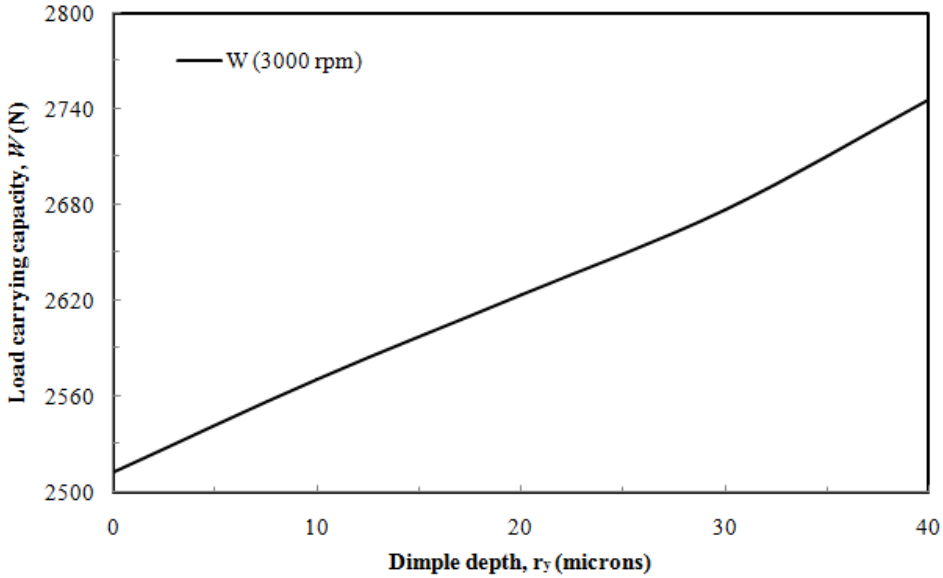

Figure 6: Effect of Dimple Depth on the Load Carrying Capacity of a Textured Porous Journal Bearing at High Shaft Speed (*N*= 3000 rpm, ε=0.3)

Table 2: Percentage Change in Load Carrying Capacity (%W) with the Variation in Dimple Depth for Low (1000 rpm) and High Speed (3000 rpm)

Dimple Depth (r_y)	% Age Change in Load (1000 rpm)(%W)	% Age Change in Load (1000rpm) (%W)
10	2.3418	2.3446
20	4.4173	4.4385
30	6.5681	6.5682
40	9.2884	9.2910

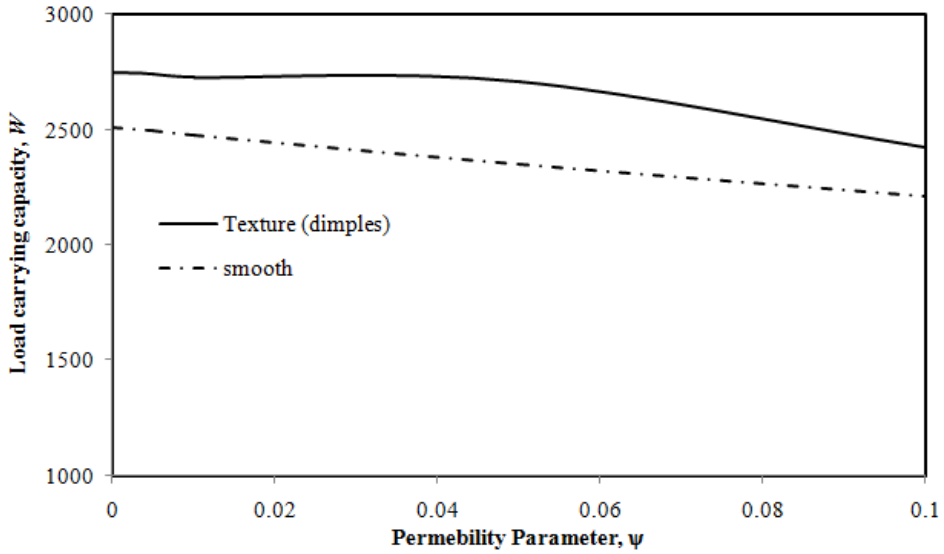

Figure 7: Effect of Permeability Parameters on the Load Carrying Capacity of a Textured and Smooth Bearing (r_y= 40 microns, *N*=3000 rpm, ε=0.3, m=0.08)

The results are also calculated for high shaft speed (3000 rpm) as depicted in Figure 6 in which same trends are obtained; the larger the depth of dimple, the load carrying capacity is higher. Results clearly shows that the texturing helps improving the bearing performance and partial texturing (0º to 128.5º) is fruitful instead of full texturing and without texturing/ smooth surface.

Moreover, the results are also calculated in the form of percentage as shown in Table 2 where percentage change in load carrying capacity is calculated. It has been observed that the shaft speed does not influences the bearing performance as at low (1000 rpm) as well as high shaft speed (3000 rpm), the percentage increase in load carrying capacity is almost same.

As the previous results reveals that large value of dimple depth and an intermediate eccentricity ratio with optimized shaft speed is advantageous for the better performance of porous journal bearing. Thus, the forthcoming results are specifically taken on the basis of previously obtained results. The investigation on the influence of permeability parameter is also an important aspect of porous bearing to be obtained. The permeability parameter is varied from 0 to 0.1 and results are calculated.

Figure 7 presents the influence of permeability parameter on the performance behavior of porous journal bearing. It has been observed that at high speed and at high value of dimple depth, the permeability parameter influences load carrying capacity as inclusion of texture enhances significantly. Moreover, the permeability parameter reduces the load carrying capacity in both cases. High value of permeability parameter reduces the load capacity at higher rate. So, an intermediate value of permeability parameter is taken (ψ=0.01) and load carrying capacity is calculated with variation of eccentricity ratio. As the applications of porous bearings are for low load and high speed. So, eccentricity is varied between 0 to 0.5 accordingly.

Conclusion

Based on the results calculated, conclusions for various bearing performance characteristics such as fluid film pressures, load carrying capacity, percentage change in load carrying capacity are presented for the effects of ellipsoidal type of textures incorporated on the bearing surface to investigate the performance of a finite porous journal bearing. The information obtained from these tables and graphs gives the following conclusions:

- The fluid film pressures developed are more pronounced as compared to the smooth bearing case with the texture effects.
- The effect of permeability parameter is to decrease the load carrying capacity and the decrement is enlarged at high values of permeability parameters.
- The location of texture is also an important parameter in improving the bearing performance as texture with full configuration (0º to 360º) and in case of divergent zone does not give fruitful results. So, the best location observed for incorporating texture is in convergent zone (0º to 128.5º).
- The load carrying capacity in cases of textured case gets improved with increase in dimple depth and decreased with increase in permeability parameter. Moreover, eccentricity ratio also improves the load carrying capacity with texture conditions.

REFERENCES

Cameron A (1966). *The Principles of Lubrication*, (Longmans, London, UK).

Gururajan K and Prakash J (1999). Surface roughness effects in infinitely long porous journal bearings. *Journal of Tribology- ASME* **121** 139-147.

Hamrock BJ, Schmid SR and Jacobson BO (2004). *Fundamentals of Fluid Film Lubrication*, 2nd edition, (Marcel Dekker, New York, USA).

Hori Y (2006). *Hydrodynamic Lubrication*, (Springer, Tokyo, Japan).

Kango S and Sharma RK (2010). Studies on the influence of surface texture on the performance of hydrodynamic journal bearing using power law model. *International Journal of Surface Science and Engineering* **4** 505-524.

Kango S, Sharma RK and Pandey RK (2014). Thermal analyses of micro-textured journal bearings using non-Newtonian rheology of lubricant and JFO boundary conditions. *Tribology International* **69** 19-29.

Kango S, Singh D and Sharma RK (2012). Numerical investigation on the influence of surface texture on the performance of hydrodynamic journal bearing. *Meccanica* **47** 469-482.

Khonsari MM and Booser ER (2001). *Applied Tribology: Bearing Design and Lubrication*, (John Wiley-Sons, New York, USA).

Kumar V (1980). Porous metal bearings - a critical review. *Wear* **63** 271-287.

Morgan VT and Cameron A (1957). Mechanism of lubrication in porous metal bearings, *Proceedings of the Conference on Lubrication and Wear, Institution of Mechanical Engineers, London* 151 - 157.

Murti PRK (1973). Lubrication of finite porous journal bearings. *Wear* **26** 95-104.

Naduvinamani NB and Patil SB (2009). Numerical solution of finite modified Reynolds equation for couple stress squeeze film lubrication of porous journal bearings. *Computers and Structures* **87** 1287-1295.

Naduvinamani NB, Hiremath PS and Gurubasavaraj G (2002). Surface roughness effects in a short porous journal bearing with a couple stress fluid. *Fluid Dynamics Research* **31** 333-354.

Prakash J and Tiwari K (1982). Lubrication of a Porous Bearing with Surface Corrugations. *Journal of Lubrication Technology- ASME* **104** 127-134.

Prakash J and Tiwari K (1983). Roughness effects in porous circular squeeze-plates with arbitrary wall thickness. *Journal of Lubrication Technology- ASME* **105** 90-95.

Reason BR and Sew AH (1985). A refined numerical solution for the hydrodynamiclubrication of finite porous journal bearings. *Institution of Mechanical Engineers-Proceedings* **199** 85-93.

Rouleau WT and Steiner LS (1974). Hydrodynamic Porous Journal Bearings. Part 1-Finite Full Bearings, *Journal of Lubrication Technology, Transactions of ASME* **96** 346-353.
Sharma N, Kango S, Sharma RK and Sunil (2014). Investigations on the effects of surface texture on the performance of a porous journal bearing operating with couple stress fluids, *International Journal of Surface Science and Engineering* **8**(4) 392-407.
Sharma N, Kango S, Tayal A, Sharma RK and Sunil (2014). Investigation on the influence of surface texturing on a couple stress fluid based journal bearing by using JFO boundary conditions. *Tribology Transactions* **59** 579-584.
Tala-Ighil N, Maspeyrot P, Fillon M and Bounif A (2007). Effects of surface texture on journal bearing characteristics under steady state operating conditions. *Proceedings of Institutions of Mechanical Engineers, Part J, Journal of Engineering Tribology* **221** 623-633.